

Experimental electronic structure and Fermi-surface instability of the correlated 3d sulphide BaVS₃: High-resolution angle-resolved photoemission spectroscopy

Mitrović, S.; Fazekas, P.; Sondergaard, C.; Ariosa, D.; Barišić, Neven; Berger, H.; Cloetta, D.; Forro, Laszlo; Hochst, H.; Kupčić, Ivan; ...

Source / Izvornik: **Physical review B: Condensed matter and materials physics, 2007, 75**

Journal article, Published version

Rad u časopisu, Objavljena verzija rada (izdavačev PDF)

<https://doi.org/10.1103/PhysRevB.75.153103>

Permanent link / Trajna poveznica: <https://um.nsk.hr/um:nbn:hr:217:248366>

Rights / Prava: [In copyright](#)/[Zaštićeno autorskim pravom.](#)

Download date / Datum preuzimanja: **2024-09-09**



Repository / Repozitorij:

[Repository of the Faculty of Science - University of Zagreb](#)



Experimental electronic structure and Fermi-surface instability of the correlated 3d sulphide BaVS₃: High-resolution angle-resolved photoemission spectroscopy

S. Mitrovic,^{1,*} P. Fazekas,^{2,3} C. S ndergaard,¹ D. Ariosa,² N. Bari i c,² H. Berger,² D. Clo etta,² L. Forr o,² H. H ochst,⁴ I. Kup ci c,^{5,2} D. Pavuna,² and G. Margaritondo^{1,2}

¹*Institut de Physique des Nanostructures, Ecole Polytechnique F d rale de Lausanne, CH-1015 Lausanne, Switzerland*

²*Institut de Physique de la Mati re Complexe, Ecole Polytechnique F d rale de Lausanne, CH-1015 Lausanne, Switzerland*

³*Research Institute for Solid State Physics and Optics, Budapest H-1525, Hungary*

⁴*Synchrotron Radiation Center, University of Wisconsin–Madison, Stoughton, Wisconsin 53589, USA*

⁵*Department of Physics, Faculty of Science, University of Zagreb, HR-10001 Zagreb, Croatia*

(Received 4 April 2007; published 19 April 2007)

The correlated 3d sulphide BaVS₃ exhibits an interesting coexistence of one-dimensional and three-dimensional properties. Our experiments determine the electronic band structure and shed light on this puzzle. High-resolution angle-resolved photoemission measurements in a 4-eV-wide range below the Fermi energy level uncover and investigate the coexistence of a_{1g} wide-band and e_g narrow-band d electrons, which lead to the complicated electronic properties of this material. We explore the effects of strong correlations and the Fermi surface instability associated with the metal-insulator transition.

DOI: [10.1103/PhysRevB.75.153103](https://doi.org/10.1103/PhysRevB.75.153103)

PACS number(s): 71.30.+h, 71.45.Lr, 79.60.–i

The correlated transition-metal sulphide BaVS₃ offers a puzzling combination of structural quasi-one-dimensionality (quasi-1D) with 3D character of some fundamental electronic and magnetic properties. Reconciling these features is a challenge for condensed-matter physics. BaVS₃ exhibits several instabilities: a structural hexagonal-to-orthorhombic transition^{1,2} at $T_S=250$ K, metal-to-insulator transition^{1,3} (MIT) at $T_{MI}=69$ K, and an onset of antiferromagnetic long-range order^{2–4} at $T_\chi=30$ K. Here we concentrate on the MIT and we present angle-resolved photoemission (ARPES) data taken at $T_\chi < T < T_S$ on both sides of the MIT. For many years, ARPES has been used to experimentally probe the electronic band structure of different materials. This powerful approach, however, requires high-quality single crystals of reasonable size. We grew suitable crystals of BaVS₃ to experimentally determine the band structure and provide a solid background for the understanding of this compound and a framework for all future studies of BaVS₃ properties.

The crystal structure can be envisaged as a triangular lattice of chains of face-sharing VS₆ octahedra, with V-V distances in the a - b plane (6.72  ) almost 2.4 times as large as in the c direction of the chains (2.84  ). Naively, one would expect this structural quasi-one-dimensionality to be reflected in the electronic structure, with high conductivity along the chain direction and poor conductivity in the perpendicular directions. If this were the case, the MIT could be driven by the tendency of quasi-1D systems to form symmetry-lowering density-wave states. Interestingly, the transport measurements on single-crystal samples reveal conductivity that is essentially isotropic ($\sigma_c/\sigma_a \sim 3$), very low in the metallic phase and only weakly dependent on temperature.³ This 3D “bad metal” conductivity in the high-temperature phase is accompanied by the Curie-Weiss-type susceptibility, indicating a substantial fraction of localized V sites.^{2,3} On the other hand, the only good candidate so far for the order parameter is 1D in character: Inami *et al.* find the doubling of the unit cell occurring in the direction of V chains,⁵ while Fagot *et al.* show that this tetramerization is

preceded by strong 1D fluctuations of the lattice in a wide temperature range above the MIT.⁶ The MIT instability is interpreted as corresponding to a charge density wave (CDW) of a 1D electron gas with a periodicity of $2k_F = 0.5c^*$.

The difficulties in understanding this coexistence of both 1D and 3D metal aspects are in large part due to the unclear character and occupancy of the low-energy electronic band structure. In the ionic picture of a single $V^{4+}=3d^1$ site, the trigonal component of the crystal field splits the t_{2g} level into a nondegenerate a_{1g} and a doubly degenerate e_g level. The a_{1g} orbitals have a z^2 character, overlapping strongly in the direction of chains. Such a band would be wide and almost 1D. If only these states were filled, we would expect to have a weakly correlated metal, or possibly a semiconductor, and no possibility for the formation of localized momenta. This is obviously not the case. There must be also e_g electrons. In fact, all band structure calculations^{7–10} agree that the Fermi energy level (E_F) is lying in the region of the crossing of a_{1g} -like and e_g -like bands. If both a_{1g} and e_g electrons are indeed present, it is important to have a clear band picture, as complicated scenarios for the MIT may arise.

We performed ARPES on fairly large ($\approx 0.25 \times 0.25 \times 3$ mm³) single crystals of BaVS₃ grown by the slow-cooling technique in melted tellurium.¹¹ The data were collected at the PGM beamline of the SRC (Stoughton, WI and with a Scienta-2002 analyzer. The spectra presented were measured with a total energy and momentum resolution of $\Delta E=15$ meV and $\Delta k=0.04$  ^{−1}. Clean surfaces were exposed in UHV conditions of the analyzer chamber (10^{-11} mbar range). The temperature of the sample could be controlled in the range from 5 to 150 K. Due to the pronounced needlelike structure, samples were fractured rather than cleaved, making the momenta of electrons poorly defined in the perpendicular directions to the one parallel to V chains. In the latter case, measurements were systematically reproducible.

Figure 1 shows the ARPES intensity map taken in the Γ -Z

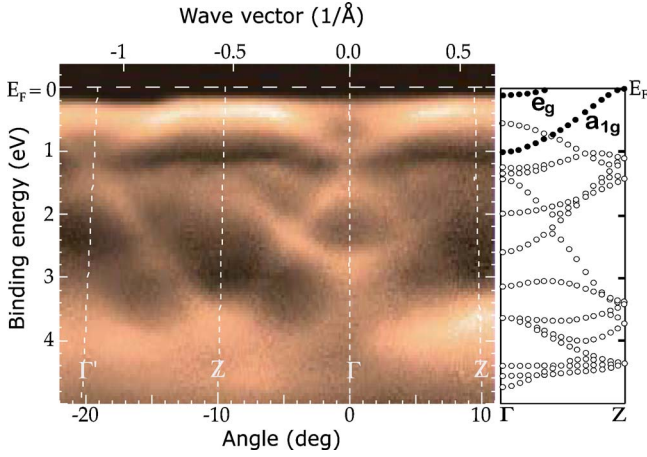


FIG. 1. (Color online) Left: ARPES intensity map at 40 K taken in the direction parallel to the structural chains. Brighter color signifies higher intensity. The spectra were normalized and a background was subtracted to enhance the features. Right: the corresponding theoretical LDA band dispersion, adopted from Ref. 10.

direction parallel to the chains. For best resolution, measurements were taken at $T=40$ K. To make the features in the vicinity of E_F distinctly resolved, we choose a photon energy of 50 eV, close to the photoionization cross section maximum for V(3d) and avoiding the high cross section for S(3p). Except for the temperature broadening and the leading edge shift close to E_F , as we discuss later, we obtain essentially the same intensity maps in the 40–150-K range. The maps reproduce the theoretical k -space periodicity in the extended zone scheme, indicating that the measurements, in fact, disclose bulk states. We read off the period $2z$ where $z=\Gamma Z \approx \pi/c_0=0.56 \text{ \AA}^{-1}$, $c_0=5.61 \text{ \AA}$ being the c -axis lattice constant for the unit cell with two V atoms. The measurement is in agreement with the latest local density approximation (LDA) calculations¹⁰ (see Fig. 1, right). Most of the bands in the 1–4-eV interval are resolved and match in width and position with the theory. The low-energy part of the spectrum ($E_B \lesssim 1$ eV), requires a more rigorous look.

The $-d^2I/dE^2$ map of Fig. 2(b) shows the details of the band structure close to E_F . We identify the dispersive band with a minimum at Γ and ~ 1 eV bandwidth as the a_{1g} band. In the absence of perpendicular-to-chain measurements, we can conclude that the a_{1g} band is at least close to quasi-1D because (i) no distinction could be found in maps of different measurements, though the perpendicular to Γ -Z orientation of the needlelike crystal was fairly arbitrary, and (ii) we obtained indistinguishably similar dispersions by varying the photon energy (25–55 eV). This band is traversed by one of the $S(\pi_z)$ bands with a maximum at Γ . We associate the seemingly flat band, just under E_F and most clearly discerned around Γ , with the e_g states. One can notice both e_g and a_{1g} bands in the plot of selected raw energy distribution curves (EDCs) presented in Fig. 2(c)

Even deep in the metallic phase ($T > T_{MI}$), the EDCs retain the width and peak positions. The width $\Delta E \sim 300$ meV is large, and the spectra are pseudogapped, with no obvious E_F crossing in the metallic phase for any of the bands. Both indicate that the observed spectral function does

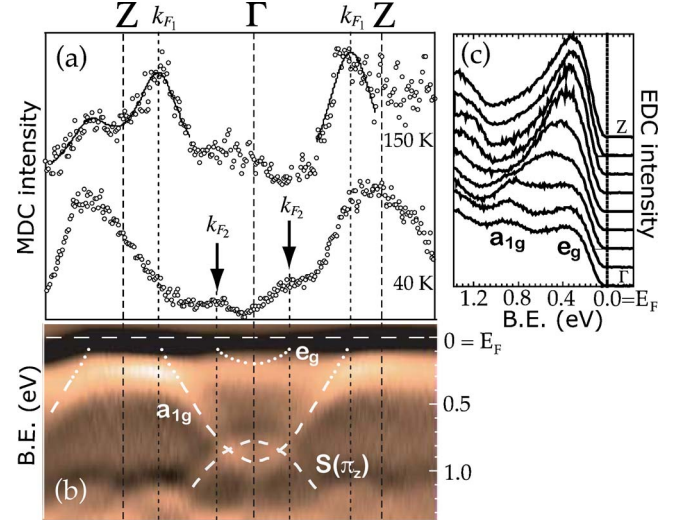


FIG. 2. (Color online) (a) An MDC of an integrated energy region $E_F < E_B < 50$ meV from an ARPES map at 150 K. A double-Lorentzian fit determines the position of k_{F1} from both sides of the BZ. Below is the equivalent MDC plot taken from a map at 40 K and 80 meV higher in binding energy to account for the gap opening (Ref. 14). The arrows indicate the positions of the second Fermi crossing, k_{F2} . (b) $-d^2I/dE^2$ plot of the ARPES map at 40 K. The white dashed and dotted lines guide the eye in following the dispersions. Refer to the text for details. (c) Selected raw EDCs in equidistant steps from the Γ to Z point, plotted with an offset.

not reflect the “bare” quasiparticle dispersion. Our angle-resolved data corroborate the results of an angle-integrated study on polycrystalline samples,¹² which reported the lack of a Fermi edge above T_{MI} . This was attributed to Luttinger liquid behavior. However, the electronic properties of BaVS₃ are far from being purely quasi-1D to permit such an interpretation. In fact, these features are not at all uncommon in systems where electrons are coupled to collective modes and are nowadays accepted as one of the signatures that carry valuable information about the interactions. They have been observed in quasi-1D metals,^{13,14} but also in high-temperature superconductors,^{15,16} layered manganites,¹⁷ and, some aspects, even in semiconductors.¹⁸

When electrons couple to collective excitations, the spectral weight on the quasiparticle peak is renormalized^{15,17} and the extent of the renormalization depends on the strength of the interactions and the dimensionality of the bands in question. If interactions are strong, almost all of the spectral weight is taken away from the quasiparticle peak. This appears to be the case in BaVS₃. Taking that into account, the dispersion map in Fig. 2(b) consists of two regions: (i) the higher-binding-energy region where EDC peak dispersion represents accurately the “frozen” lattice dispersion (dashed lines as guides to the eye) and (ii) the region between E_F and the closest EDC peak—whose position is determined by interactions—where we observe only flat features (dotted lines as guides to the eye). Nevertheless, the dispersing quasiparticle spectrum is there, and this is directly observable in momentum distribution curves (MDCs). MDCs are equivalent to EDCs, but with the advantage of being less sensitive to interactions.¹⁶

In Fig. 2(a) we plot an MDC around the E_F from an ARPES map taken in the metallic phase. The Lorentzian-shaped peaks are a token of quasiparticles. They disclose the E_F crossings of the a_{1g} band within the first and second Brillouin zones (BZs). The value from Lorentzian peak fits of the wave vector $k_{F_1} = (0.40 \pm 0.05) \text{ \AA}^{-1}$ is in good agreement with the latest theoretical result, which includes interactions in the band picture, specifically Fig. 4 of Ref. 10. As for the e_g states, there is only a slight increase of intensity not far from the Γ point in the MDC of Fig. 2(a), which could indicate a crossing of a predicted electron pocket.^{9,10} For better resolution we need to look at the map at a lower temperature (40 K), but to have equivalency of MDCs we take one at higher binding energy to account for the gap opening Δ_{ch} .¹⁴ We determine the gap value directly from our spectra, as we describe later. Since we are able to fit the same width and position Lorentzians for a_{1g} peaks, we trust the correctness of this procedure. The two new peaks that are revealed are symmetric around the Γ point and indicate an electron pocket crossing E_F at $k_{F_2} = (0.15 \pm 0.05) \text{ \AA}^{-1}$. This is again in good agreement with the value from Ref. 10. Unlike for a_{1g} , where we can follow the dotted part of the dispersion by plotting successive MDCs, we cannot do the same for e_g states. The dotted line in Fig. 2(b) is only for illustration purposes; the actual states are too narrow to be revealed in MDCs.

If the Lorentzian peaks in MDCs may truly be regarded as quasiparticles, they should reveal the real gap and show the phase transition. If we plot the position of the leading edge of measured spectral functions versus temperature, we see a monotonic shift—which most likely started above 150 K—and a noticeable nonlinear increase in the shift below 90 K. This is consistent with the results of Ref. 12 and indicative of the opening of a charge gap. We do not see a clear transition associated with the $T_{MI} = 69$ K. This is not unusual, particularly in CDW systems when pretransitional fluctuations are present or in systems where conducting, wide-band electrons are strongly scattered by the narrow-band electrons and/or by the localized states placed at energies close to E_F . The gap as seen in photoemission spectra develops in the same range of temperatures where resistivity^{3,19} identifies a “precursor” to the insulating phase and where x-ray diffraction detects large 1D fluctuations.⁶ The saturation of the leading edge shift indicates a charge gap of $\Delta_{ch} = 60\text{--}70$ meV. This is about the same value as the full charge gap from transport measurements.^{2,3,12}

We examined our experimentally determined band structure to identify a Fermi surface instability which can introduce a gap into the wide a_{1g} band. We find that the a_{1g} band alone cannot satisfy the nesting condition as $2k_{F_1} > Q_{CDW} = 0.5c^*$. An intraband nesting of a half-filled a_{1g} band would be most prominent in the Γ -Z direction, where strong 1D fluctuations are observed,⁶ so it is expected to be discerned in our intensity maps. Therefore, we may conclude that this scenario is not likely for this compound. On the other hand, our results tempt us to consider an instability involving both bands, since our data are in agreement with the condition $k_{F_1} + k_{F_2} = Q_{CDW}$. In this scenario the whole Fermi surface is removed. This is confirmed in the temperature dependence presented in Fig. 3 because we observe the same evolution at

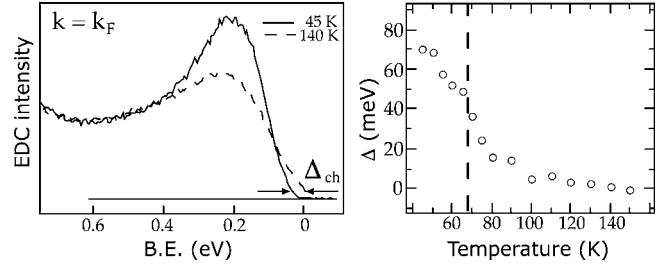


FIG. 3. Left: EDCs at $k = k_{F_1}$ taken at 140 and 45 K. The charge gap is observable in the shift of the leading edge, where the actual quasiparticle is situated. Right: the shift of the leading edge as a function of temperature. The dashed line in (right) marks the MIT temperature.

both k_{F_1} and k_{F_2} . The gap opens across the entire Fermi surface. However, this scenario cannot be fully reconciled with, at least, the x-ray diffraction experiments. Therefore, the nature of the exact mechanism for the MIT remains an open question, but it must include both bands.

ARPES cannot see the empty part of the a_{1g} band, but judging from the occupied part, its overall width must approach the theoretical value $W(a_{1g}) \geq 2$ eV.^{9,10} On the other hand, the width of the e_g band is very small, as discussed above. We conclude that the intriguing behavior of BaVS_3 results from the fact that two kinds of d states, strongly correlated narrow-band e_g states and weakly correlated wide-band a_{1g} states, coexist at the Fermi level. The isotropic, highly localized, e_g band explains the Curie-like susceptibility. Lechermann *et al.* provide the only theoretical work that correctly describes the band structure that we obtain experimentally, by including the correlations¹⁰ and show that the population between the bands is split with the ratio $n(a_{1g}) : n(e_g) \cong 1/2 : 1/2$. Therefore, exactly half of the electrons are localized. Small anisotropy in transport is observed as the quasi-1D a_{1g} -band influence is reduced through a certain combination of e_g - a_{1g} scattering, hybridization with sulphur bands, or likely electron-phonon interaction. In fact, the width of the quasiparticle peaks in MDCs allows for the direct determination of the coherence length $\Delta\ell \cong (9.7 \pm 0.4) \text{ \AA}$. This value is smaller than two unit cells and explains why the conductivity is much lower in the $T > T_{MI}$ phase than it would be in a normal metal.

To conclude, we measure the electronic band structure by ARPES in a wide range of temperatures on both sides of the MIT. We find discernible quasiparticle features, even though the spectral function is profoundly influenced by strong interactions. Our results show that the physics of BaVS_3 is governed by the coexistence of weakly correlated wide-band a_{1g} electrons and strongly correlated narrow-band e_g electrons near the Fermi energy level. Both bands must be considered to explain the observed 1D instability,⁶ as the examined points of the Fermi surface do not support the intraband nesting of the half-filled a_{1g} band and the charge gap opens over the entire Fermi surface, involving both bands.

The authors thank T. Fehér and S. Barišić for illuminating discussions. Initial measurements were performed at ISA,

University of Aarhus, Denmark, and we are grateful to P. Hofmann for this opportunity. This work is based upon research conducted at the Synchrotron Radiation Center, University of Wisconsin-Madison, which is supported by the Na-

tional Science Foundation under Grant No. DMR-0537588. P.F. acknowledges support by Hungarian National Grant No. T038162. This work was supported by the Swiss National Science Foundation through the MaNEP NCCR.

*Present address: California Institute of Technology, Department of Physics, Pasadena, CA 91125.

Electronic address: mitrovic@caltech.edu

¹O. Massenet, R. Buder, J. J. Since, C. Schlenker, J. Mercier, J. Kelber, and D. G. Stucky, *Mater. Res. Bull.* **13**, 187 (1978).

²T. Graf, D. Mandrus, J. M. Lawrence, J. D. Thompson, P. C. Canfield, S. W. Cheong, and L. W. Rupp, *Phys. Rev. B* **51**, 2037 (1995).

³G. Mihály, I. Kezsmarki, F. Zamborszky, M. Miljak, K. Penc, P. Fazekas, H. Berger, and L. Forró, *Phys. Rev. B* **61**, R7831 (2000).

⁴H. Nakamura, T. Yamasaki, S. Giri, H. Imai, M. Shiga, K. Kojima, M. Nishi, K. Kakurai, and N. Metoki, *J. Phys. Soc. Jpn.* **69**, 2763 (2000).

⁵T. Inami, K. Ohwada, H. Kimura, M. Watanabe, Y. Noda, H. Nakamura, T. Yamasaki, M. Shiga, N. Ikeda, and Y. Murakami, *Phys. Rev. B* **66**, 073108 (2002).

⁶S. Fagot, P. Foury-Leylekian, S. Ravy, J. P. Pouget, and H. Berger, *Phys. Rev. Lett.* **90**, 196401 (2003).

⁷L. F. Mattheiss, *Solid State Commun.* **93**, 791 (1995).

⁸X. Jiang and G. Y. Guo, *Phys. Rev. B* **70**, 035110 (2004).

⁹M.-H. Whangbo, H. J. Koo, D. Dai, and A. Villesuzanne, *J. Solid State Chem.* **165**, 345 (2002); *J. Solid State Chem.* **175**, 384 (2003).

¹⁰F. Lechermann, S. Biermann, and A. Georges, *Phys. Rev. Lett.* **94**, 166402 (2005).

¹¹H. Kuriyaki, H. Berger, S. Nishioka, H. Kawakami, K. Hirakawa, and F. A. Levy, *Synth. Met.* **71**, 2049 (1995).

¹²M. Nakamura, A. Sekiyama, H. Namatame, A. Fujimori, H. Yoshihara, T. Ohtani, A. Misu, and M. Takano, *Phys. Rev. B* **49**, 16191 (1994).

¹³K. E. Smith, K. Breuer, M. Greenblatt, and W. McCarroll, *Phys. Rev. Lett.* **70**, 3772 (1993).

¹⁴L. Perfetti, S. Mitrovic, G. Margaritondo, M. Grioni, L. Forró, L. Degiorgi, and H. Hochst, *Phys. Rev. B* **66**, 075107 (2002).

¹⁵G. A. Sawatzky, *Nature (London)* **342**, 480 (1989).

¹⁶A. Kaminski, M. Randeria, J. C. Campuzano, M. R. Norman, H. Fretwell, J. Mesot, T. Sato, T. Takahashi, and K. Kadowaki, *Phys. Rev. Lett.* **86**, 1070 (2001).

¹⁷D. S. Dessau, T. Saitoh, C.-H. Park, Z.-X. Shen, P. Villeda, N. Hamada, Y. Moritomo, and Y. Tokura, *Phys. Rev. Lett.* **81**, 192 (1998).

¹⁸S. Mitrovic, L. Perfetti, C. Søndergaard, G. Margaritondo, M. Grioni, N. Barišić, L. Forró, and L. Degiorgi, *Phys. Rev. B* **69**, 035102 (2004).

¹⁹L. Forró, R. Gaal, H. Berger, P. Fazekas, K. Penc, I. Kezsmarki, and G. Mihaly, *Phys. Rev. Lett.* **85**, 1938 (2000).